The molecular pathogenesis of superoxide dismutase 1-linked ALS is promoted by low oxygen tension

Isil Keskin[1], Elin Forsgren[2], Manuela Lehmann[2], Peter M. Andersen[2], Thomas Brännström[1], Dale J. Lange[3], Matthis Synofzik[4,5], Ulrika Nordström[2], Per Zetterström[6], Stefan L. Marklund[6,*] & Jonathan D. Gilthorpe[2,**]

1 Department of Medical Biosciences Pathology, Umeå University, 90185 Umeå, Sweden
2 Department of Pharmacology and Clinical Neuroscience, Umeå University, 90187 Umeå, Sweden
3 Department of Neurology, Hospital for Special Surgery and Weill Cornell Medical Center, New York, NY, USA
4 Department of Neurodegenerative Diseases, Hertie Institute for Clinical Brain Research, University of Tübingen, Germany
5 German Research Center for Neurodegenerative Diseases (DZNE), 72076 Tübingen, Germany
6 Department of Medical Biosciences, Clinical Chemistry, Umeå University, 90185 Umeå, Sweden
*Corresponding author. Tel: +46 90 7851239; E-mail: stefan.marklund@umu.se
**Corresponding author. Tel: +46 90 7854439; E-mail: jonathan.gilthorpe@umu.se

Abstract

Mutations that destabilize superoxide dismutase 1 (SOD1) are a cause of amyotrophic lateral sclerosis (ALS). SOD1, which is located in the reducing cytosol, contains an oxidized disulfide bond required for stability. We show that the bond is an Achilles heel of the protein because it is sensitive to the oxygen tension. Culture of ALS patient-derived fibroblasts, astrocytes and induced pluripotent stem cell-derived mixed motor neuron and astrocyte cultures (MNACs) under lowered oxygen tensions caused reductive bond cleavage and misfolding. The effects were greatest in cells expressing mutant SOD1s, but also occurred in wild type SOD1 in cultures derived from patients carrying ALS-linked mutations in *C9orf72*, *FUS* and *TBK1*, as well as from controls. MNACs showed a greater response than the other cell types, including enhanced SOD1 aggregation, in line with the vulnerability of the motor system. Our results show that oxygen tension is a principal determinant of SOD1 stability and shed light on how risk factors for ALS, such as aging and other conditions causing reduced vascular perfusion, could lead to disease initiation and progression.

Running title Low oxygen drives SOD1 aggregation

Keywords Amyotrophic lateral sclerosis; disulfide bond; oxygen; protein aggregation; superoxide dismutase 1

Subject categories Neuroscience; Molecular Biology of Disease

Introduction

Amyotrophic lateral sclerosis (ALS) is characterized by adult-onset progressive degeneration of upper and lower motor neurons (MN) and their associated tracts. Usually the disease begins focally and then spreads contiguously, resulting in progressive paralysis and death from respiratory failure (Charcot, 1873). Mutations in the gene encoding the ubiquitously expressed, free radical scavenging enzyme superoxide dismutase 1 (SOD1) cause ALS (Rosen et al., 1993), and are found in 1-9% of patients (Andersen & Al-Chalabi, 2011). Of over 200 mutations identified, 174 are missense and result in SOD1 variants of which most in large, although variable proportions are natively folded (Andersen et al., 1995, Sato et al., 2005, Synofzik et al., 2012). Twenty-seven encode mutants with disruptive changes (insertions, deletions and truncations) that impede native folding. Most of the truncated mutants lack C146 and thereby the C57-C146 disulfide bond, which is critical for SOD1 stability. These mutants are highly unstable and rapidly degraded (Birve et al., 2010, Jonsson et al., 2004, Keskin et al., 2017, Keskin et al., 2016, Sato et al., 2005). Hence, the collective genetic and biochemical evidence from patients infers that any common ALS-causing SOD1 species is disordered, lacks the C57-C146 disulfide bond and is only present in minute amounts.

Neuronal inclusions containing aggregated SOD1 are a hallmark of ALS, both in patients and in transgenic (Tg) animal models expressing mutant human SOD1s (Kato et al., 2000). We have shown that two structurally distinct strains of SOD1 aggregates form in Tg mouse models (Bergh et al., 2015), and that both transmit spreading, templated SOD1 aggregation and fatal ALS-like disease in a prion-like manner (Bidhendi et al., 2016). Similarly, others have shown seeding effects of spinal cord extracts from end-stage SOD1 Tg mice (Ayers et al., 2014, Ayers et al., 2016). The templated growth of SOD1 aggregation depends on disordered, disulfide-reduced SOD1 species as building blocks (Chattopadhyay et al., 2008, Chattopadhyay et al., 2015, Furukawa et al., 2008, Lang et al., 2012). This could represent the core pathogenic mechanism in SOD1-induced ALS.

Human SOD1 is primarily localized in the cytosol and is composed of two equal 153 amino acid-long subunits, each containing 1 Cu and 1 Zn ion as well as the stabilizing C57-C146 disulfide bond. SOD1 is an ancient enzyme and was secreted to the oxidizing extracellular/periplasmic space in early unicellular organisms, as well as in current α-bacteria (Bordo et al., 1994, Miller, 2012). However, the cytosol is strongly reducing and the C57-C146 bond could be an evolution-related Achilles heel of eukaryotic SOD1, and a critical

84 determinant of its role in ALS. Absence of the disulfide bond promotes misfolding and
85 aggregation of SOD1 *in vitro* (Chattopadhyay et al., 2008, Chattopadhyay et al., 2015,
86 Furukawa et al., 2008, Keskin et al., 2016, Lang et al., 2012). Moreover, aggregated as well as
87 soluble misfolded SOD1 species in the central nervous system (CNS) of SOD1 Tg models
88 lack the bond (Bergemalm et al., 2010, Karch et al., 2009, Zetterström et al., 2013,
89 Zetterstrom et al., 2007).
90 If the C57-C146 disulfide bond in SOD1 were in equilibrium with reduced and oxidized
91 glutathione (GSH/GSSG) - the principal redox couple in the cytosol - it would be almost
92 completely reduced (Mercatelli et al., 2016, Schwarzlander et al., 2016). Instead, the status of
93 C57-C146 seems to be determined kinetically with oxidation provided by O_2 and catalyzed by
94 copper chaperone for SOD (CCS) (Culotta et al., 1997, Fetherolf et al., 2017, Furukawa et al.,
95 2004). Reduction is provided by glutaredoxin-1 using reducing equivalents from GSH
96 (Carroll et al., 2006). Thus, cellular O_2 tension might be a major determinant of SOD1
97 disulfide bond stability.
98 Age is the principal non-hereditary risk factor for ALS, as well as most other
99 neurodegenerative diseases. It is associated with reduced perfusion in the CNS owing to
100 vascular wall degeneration and neurovascular unit dysfunction (Iadecola, 2017). We
101 hypothesized that local reductions in O_2 tension caused by impaired perfusion may have an
102 effect on SOD1 stability. To test this idea we used *in vitro* cell culture models of ALS
103 including fibroblasts from ALS patients carrying mutations in *SOD1*, other ALS-linked genes
104 and from non-disease controls. We also examined neural cells including primary patient-
105 derived astrocytes and mixed motor neuron and astrocyte cultures (MNACs) derived from
106 induced pluripotent stem cells (iPSCs). We found that low O_2 tensions markedly increased
107 disulfide bond reduction, misfolding and aggregation of SOD1 in a time- and concentration-
108 dependent manner.
109

110 # Results

111 ## Low oxygen tensions promote misfolding of SOD1 in patient-derived cells

112 Previously, we have utilized ALS patient-derived dermal fibroblasts as an *in vitro* model to
113 study misfolding under physiological SOD1 expression levels (Keskin et al., 2016). Cells
114 cultured *in vitro* are typically maintained in humidified ambient air supplemented with 5%
115 (v/v) CO_2, resulting in an O_2 tension of approximately 19%. However, under normal

conditions the O_2 tension in the CNS is much lower, ranging between 0.2 and 5% (Erecinska & Silver, 2001, Lyons et al., 2016). Moreover, an age-related disruption in perfusion might lead to further reductions in local O_2 tensions. Therefore, we examined the SOD1 misfolding response in fibroblast lines carrying ALS-linked *SOD1* mutations and cultured at reduced O_2 tensions for 24 h (Fig 1A and Table EV1).

Misfolded SOD1 was quantified with a specific ELISA (misELISA) (Zetterström et al., 2011). Lines carrying the $SOD1^{N86S}$ and $SOD1^{E78\_R79insSI}$ mutations showed distinct O_2 concentration responses, with the highest levels of misfolding detected at 1% O_2 (Fig 2A). Interestingly, no increase in SOD1 misfolding was seen in a line carrying the $SOD1^{G127Gfs*7}$ (G127X) truncating mutation, which results in a protein that lacks the C57-C146 disulfide bond and cannot fold properly (Fig 2A and Fig EV1A).

We next investigated the temporal response of misfolding to low O_2 and detected a significant increase in misfolded SOD1 at 1% O_2 after 4 h, reaching a maximum after 8 h, which was maintained at 24 h (Fig 2B). Quantification of total SOD1 revealed that increased misfolding was not due to increased SOD1 expression (Fig EV1B). To address whether the increase in misfolding was reversible, we quantified misfolded SOD1 at different time points after returning cells from 24 h at 1% O_2 to 19% O_2. A rapid reversal was observed in the $SOD1^{G93A}$ line with a misfolded SOD1 half-life of ~15 min, returning to baseline after ~1 h (Fig 2C). Reversal of misfolding of wild-type SOD1 ($SOD1^{WT}$) in a control line was even more rapid (Fig 2C). No significant effects were seen in the $SOD1^{G127X}$ line (Fig 2C). Hence, we concluded that the misfolding response was inversely proportional to the O_2 tension. It was also time-dependent, reversible, and appeared to require the C57-C146 disulfide bond.

To probe the misfolding response in more detail, we next analyzed a panel of control and patient-derived fibroblast lines cultured under conditions where the misfolding response was maximal (1% O_2, 24 h; Fig 2D and Fig EV1C). A significant increase in misfolded SOD1 was seen in all lines that carried full-length mutant SOD1s and ranged from 1.5 – 3.5-fold. Significant increases of a smaller magnitude were also observed in most control lines, as well as those from patients carrying ALS-linked *C9orf72*, *FUS* or *TBK1* mutations, which only contain $SOD1^{WT}$. The only fibroblasts that did not show significant increases were lines carrying *SOD1* mutations resulting in truncations and the absence of C146*:* $SOD1^{G127X}$ and $SOD1^{D125Tfs*24}$.

To investigate the misfolding response in patient-derived neural cells, we generated primary astrocytes from the lateral ventral horn of an ALS patient heterozygous for the $SOD1^{A4V}$ mutation (Fig 1A, Fig 2E, Fig EV1 D and E and Table EV1) (Haidet-Phillips et al.,

2011). The level of misfolded SOD1 increased 2-fold when these cells were cultured at 1% O_2 compared to 19% for 24 h (Fig 2E and Fig EV1D), which was similar to the increase seen in fibroblasts from another *SOD1*^{A4V} patient (Fig 2D and Fig EV1C).

An enhanced SOD1 misfolding response in patient-derived motor neuron/astrocyte cultures

Since ALS preferentially targets the motor system, we reprogrammed a subset of the patient-derived fibroblast lines to iPSCs and differentiated these to MNACs (Fig 1A and B and Table EV1). Recently we have found that SOD1 misfolding is enhanced in MNACs compared to the corresponding fibroblasts, iPSCs and iPSC-derived sensory neurons (Forsgren et al., under revision). After 10 days in culture post-differentiation (Day 25; Fig 1B), MNACs contained ~5% neurons expressing tubulin beta 3 class III (TUBB3; Fig EV2 A and B). A large proportion of these neurons (78 – 84%) co-expressed the motor neuron markers ISL LIM homeobox 1/2 (ISL1/2) and non-phosphorylated neurofilament-H (SMI32), representing a limb innervating subtype that are highly susceptible to ALS (Amoroso et al., 2013).

We first titrated the dose-response of SOD1 misfolding to O_2 tension in MNACs from control, SOD1^{A4V} and SOD1^{G93A} lines. A significant increase in misfolding was detected at ≤4% and was maximal at 2% O_2, which was enhanced in MNACs compared to fibroblasts in all three lines (Fig 3A). Under the same conditions used for fibroblasts (1% O_2 for 24 h), a significant degree of axonal fragmentation was observed (data not shown), indicative of neuronal stress. However, since axonal morphology (Fig EV2B), cellular ATP levels (Fig EV3A) and viability (Fig EV3B) were not significantly affected by exposure to 2% O_2 for 24 h, this was used to investigate the misfolding response in MNACs from ALS patients.

Large increases in SOD1 misfolding, ranging up to 10-fold, were induced in MNACs following exposure to 2% O_2 for 24 h (Fig 3B and Fig EV4). The largest effects were found in several of the lines expressing full-length mutant SOD1s (N86S, A4V, and G93A). However, in contrast to fibroblasts a robust 3 – 4-fold increase was also seen in controls expressing SOD1^{WT} and in MNACs that were heterozygous for *SOD1*^{G127X} or *SOD1*^{D125Tfs*24} mutations. This is likely to represent enhanced misfolding of SOD1^{WT} in MNACs (Forsgren et al., under revision), since the level of mutant protein did not increase in the SOD1^{G127X} line (Fig EV5).

Our previous study of patient-derived fibroblasts showed that misfolded SOD1 is primarily degraded by the proteasome (Keskin et al., 2016). However, exposure to low O_2 tension did

not lead to a reduction in proteasome activity in MNAC extracts (Fig EV3C). Nor were there increases in $SOD1^{G127X}$ protein in either soluble (Fig EV5) or detergent-insoluble (Fig EV6B) fractions, which both increased greatly upon proteasome inhibition (Keskin et al., 2016). Inhibition of the proteasome also leads to copious aggregation of $SOD1^{D125Tfs*24}$ in fibroblasts (Keskin et al., 2016), whereas no changes were found here in response to low O_2 tension (see below; Fig 7). Hence, increased SOD1 misfolding at low O_2 tension could not be attributed to a reduction in proteasome activity.

Low oxygen tension promotes reductive cleavage of the disulfide bond

We have shown that reduction of the C57-C146 bond is a prerequisite for SOD1 misfolding in the CNS (Zetterström et al., 2013, Zetterstrom et al., 2007). To examine the status of the disulfide bond in MNACs we determined the proportions of disulfide-reduced and oxidized SOD1 by non-reduced western blotting (Fig 4A and B). Culture at 2% O_2 for 24 h resulted in significant increases in disulfide-reduced SOD1, both in control lines expressing $SOD1^{WT}$ and those expressing mutant SOD1s. However, this was not the case for the $SOD1^{H46R}$ line, where a large proportion of the mutant protein is known to be disulfide-reduced under control conditions (Winkler et al., 2009).

Misfolded SOD1 in MNACs lacks the disulfide bond

To confirm that misfolded SOD1 lacks the C57-C146 disulfide bond, we immunocaptured SOD1 from extracts of MNACs, which had been cultured at 19% or 2% O_2, using the same antibody (SOD1 aa 24-39) and capture conditions (1 h at 23°C) used in the misELISA. This antibody reacts with disordered SOD1, independent of the C57-C146 disulfide status (Forsberg et al., 2010). Disulfide-reduced and oxidized SOD1 were quantified by non-reduced western blotting (Fig 4C). Input samples from control, $SOD1^{G93A}$ and $SOD1^{A4V}$ MNACs contained a majority of oxidized and a small proportion of reduced SOD1, which increased at low O_2 conditions. Notably, the misfolded SOD1-specific antibody only captured disulfide-reduced SOD1. In control MNACs, this was not detectable at 19% O_2 but increased at 2% O_2 to ~1.4% of the disulfide reduced SOD1 in the input sample. In $SOD1^{G93A}$ and $SOD1^{A4V}$ MNACs, immunocaptured disulfide reduced misfolded SOD1 increased substantially (to 21% and 10% of the input samples at 2% O_2, respectively). Hence, in patient-derived MNACs, the majority of disulfide-reduced SOD1 retained an ordered structure. This agrees with

observations in the spinal cord of SOD1 Tg mouse models, where approximately 5 – 10% of disulfide-reduced human SOD1 is disordered (Zetterström et al., 2013, Zetterstrom et al., 2007).

Low oxygen tension does not alter determinants of SOD1 redox status

Oxidation of the C57-C146 disulfide bond is catalyzed by CCS (Culotta et al., 1997, Fetherolf et al., 2017, Furukawa et al., 2004), and it can be reduced by a mechanism involving reducing equivalents from GSH via glutaredoxin-1 (Carroll et al., 2006). To determine whether these factors were affected by low O_2 tension and responsible for increased misfolding, we analyzed their levels in MNACs grown at 19% vs 2% O_2. No significant changes were detected in CCS or glutaredoxin-1 levels by western blotting (Fig 5A and B and Fig EV7). We next quantified GSH and GSSG in MNACs and fibroblasts (Fig 5C and *D)*. GSH and GSSG concentrations were higher in MNACs than in fibroblasts, but exposure to low O_2 tension did not lead to significant changes in GSH or GSSG levels. The concentrations of GSSG were remarkably high in MNACs, resulting in very low GSH/GSSG ratios, but these were not affected by O_2 (Fig 5E). Hence, low O_2 tensions do not induce disulfide reduction and misfolding of SOD1 via gross perturbations of the GSH/GSSG redox couple (Schwarzlander et al., 2016).

Maintenance of the disulfide bond and SOD1 structure is oxygen-dependent

Increased misfolding at low O_2 tension could be due to impaired disulfide oxidation of newly synthesized SOD1, or to reduction of the disulfide bond in the mature protein. To distinguish the relative contribution of these two possible mechanisms, we compared the misfolding response in fibroblasts cultured in the absence or presence of the protein synthesis inhibitor cycloheximide (CHX) for 24 h. No significant effect of CHX on the level of misfolded $SOD1^{WT}$ was seen in control fibroblasts cultured at 19% or 1% O_2 (Fig 6A). In contrast, CHX treatment led to a large reduction in misfolded SOD1 in the $SOD1^{G127X}$ line at both O_2 tensions (Fig 6B). This confirmed that both the inhibition of protein synthesis, and the degradation of the disordered $SOD1^{G127X}$ mutant protein, was efficient. In the $SOD1^{G93A}$ line, CHX treatment resulted in a significant reduction in misfolded SOD1 at both O_2 tensions. Hence, a proportion of misfolded SOD1 resulted from a lack of disulfide oxidation in newly synthesized $SOD1^{G93A}$ (Fig 6C). However, the misfolding response was enhanced at 1%

compared to 19% O_2 even when protein synthesis was inhibited. Thus, O_2 is also required for maintenance of the disulfide bond and structure of the existing pool of mature SOD1.

Low oxygen tension promotes SOD1 aggregation

Since disulfide reduction and misfolding promote SOD1 aggregation (Chattopadhyay et al., 2008, Furukawa et al., 2008, Lang et al., 2012), we quantified detergent-resistant SOD1 aggregates in both fibroblasts and MNACs. Low levels of aggregation were found in fibroblasts, which did not increase significantly in response to low O_2 (Fig 7). In contrast, we found that low O_2 tension induced marked increases in aggregation in MNACs carrying full-length mutant SOD1s (E78_R79insSI, N86S, G93A and A4V), but not in $SOD1^{WT}$ control lines or $SOD1^{L117V}$, which has $SOD1^{WT}$-like stability (Synofzik et al., 2012). The $SOD1^{H46R}$ mutation disrupts copper binding catalyzed via CCS and impairs formation of the disulfide bond (Winkler et al., 2009). In agreement, the high level of aggregation present at 19% O_2 in the $SOD1^{H46R}$ line did not change at 2% O_2. Neither of the lines expressing the C-terminally truncated mutants that lack the disulfide bond ($SOD1^{G127X}$ and $SOD1^{D125Tfs*24}$), showed increased aggregation. Hence, increased aggregation correlated closely with increased misfolding in MNACs expressing full-length mutant SOD1s.

Discussion

The principal finding of this study is that culture at low O_2 tension leads to remarkably large increases in SOD1 C57-C146 disulfide bond reduction and misfolding. In addition to being required for bond formation, we have identified that O_2 is also critical for its maintenance. Low O_2 tension resulted further in enhanced aggregation in MNACs but not in fibroblasts. This supports the idea that in human patient-derived models, as well as in Tg mice, the C57-C146 disulfide bond is indeed an ALS-related Achilles heel of SOD1 in the reducing environment of the cytosol.

The O_2 tensions in the gas phase found to enhance SOD1 misfolding are within the range considered to be normoxic in human and animal tissues. However, the range of O_2 tensions present within cultured cells are likely to be lower. This is due to both the rate of O_2 diffusion through the culture medium and the rate of O_2 consumption by cellular respiration, which depends on both cellular mass and the rate of oxidative metabolism (Pettersen et al., 2005). Because these variables are difficult to control for between different cell lines, we chose to

compare replicate samples cultured at different O_2 tensions. The cells, which had been propagated and adapted to growth at 19% O_2, were tested within a range that was found not to cause overt toxicity.

A study in young resting awake mice has indicated that O_2 tensions in the CNS vary between 0.2 – 5% (Lyons et al., 2016). Even lower levels were recorded under normal conditions, e.g. in periarteriolar areas. Considering this great variation found in young mice, it is reasonable to assume that localized hypoxia could occur transiently, or more chronically, in elderly humans even in the absence of overt disease.

Apart from the strong risk associated with aging, other suggested non-hereditary risk factors for ALS include smoking (Gallo et al., 2009), CNS trauma, particularly to the motor cortex (Rosenbohm et al., 2014), embolisations of arteriovenous malformations, transient ischaemic attack, and stroke (Turner et al., 2016). Strenuous physical activity has also been suggested to increase the risk for ALS (Chio et al., 2005), although this is contentious (Gallo et al., 2016). The mechanisms underlying these risk factors are not understood, but a unifying characteristic could be transient or chronic CNS hypoxia due to reduced vascular perfusion.

In *SOD1* ALS mouse models, the average lifespan of homozygous Tg mice is approximately half that of hemizygous animals (Jaarsma et al., 2000, Jonsson et al., 2004). A dose-dependence on mutant SOD1s also exists for the development of ALS in humans. Individuals that are homozygous for the *SOD1* mutations L84F, N86S or L126S show earlier onset and more rapid progression than those that are heterozygous for the same mutation (Alavi et al., 2013, Boukaftane et al., 1998, Hayward et al., 1998, Kato et al., 2001). Furthermore, the D90A mutant protein, which has wild type-like stability, typically only causes ALS in homozygous individuals (Andersen et al., 1996). Hence, a clear link exists between a doubling of the load of mutant SOD1 and disease initiation, or progression. The large increases in misfolded SOD1 in response to low O_2 tension we report here, particularly in MNACs, could contribute to the initiation and progression of ALS.

Except for $SOD1^{D90A}$, the cell lines tested here were derived from individuals heterozygous for *SOD1* mutations. Whereas $SOD1^{D90A}$ has a larger electrophoretic mobility, the other full-length SOD1 mutants show the same mobility as wild-type SOD1. The $SOD1^{D125Tfs*24}$ mutant protein also has the same mobility as $SOD1^{WT}$ (Keskin et al., 2016). Therefore, these SOD1 mutants cannot be distinguished from $SOD1^{WT}$ by western blotting or in the misELISA (Keskin et al., 2016). Owing to widely different stabilities and rates of degradation, the levels of mutant SOD1s in cultured human cells vary from comparable to the wild type protein, to very low (Keskin et al., 2016). Whereas there were no large differences in the proportion of

disulfide-reduced SOD1 between *SOD1* mutant and control MNACs, both basal and low O_2-enhanced levels of misfolded and aggregated SOD1 were much greater in the *SOD1* mutant cultures. For the most part, mutant SOD1s most likely contributed substantially to these enhanced levels.

Recent findings *in vivo* suggest that prion-like growth and spread of SOD1 aggregation could be the primary disease mechanism of SOD1-induced ALS (Ayers et al., 2014, Ayers et al., 2016, Bidhendi et al., 2016). Disordered SOD1 species would be critical substrates for both the nucleation and growth of prion-like aggregates. This would have a greater probability of occurring in areas of the CNS with sustained low O_2 tension. Consistent with this, even a short (24 h) exposure to low O_2 tension resulted in large increases in SOD1 aggregation in patient-derived MNACs, which do not overexpress the protein. Typically SOD1 overexpression is required for substantial aggregation to occur (Prudencio et al., 2009).

Significant increases in disulfide-reduced and misfolded SOD1 were also seen in cells from healthy control individuals and cells derived from patients carrying ALS-linked mutations in other genes. This could be important since there is mounting evidence for involvement of $SOD1^{WT}$ in ALS patients without *SOD1* mutations. Although this is debated (Da Cruz et al., 2017), several studies have demonstrated inclusions of misfolded $SOD1^{WT}$ in the soma of motor neurons from sporadic as well as familial ALS patients carrying ALS-linked mutations in other genes (Bosco et al., 2010, Forsberg et al., 2011, Forsberg et al., 2010, Pokrishevsky et al., 2012). Furthermore, co-culture of motor neurons with primary astrocytes derived from sporadic ALS patients indicates an involvement of $SOD1^{WT}$ in the disease (Haidet-Phillips et al., 2011), and mice that express human $SOD1^{WT}$ at high rate develop both SOD1 aggregation and a fatal ALS-like disease (Graffmo et al., 2013).

SOD1s carrying mutations that affect the C57-C146 disulfide bond should not be affected directly by low O_2 tension. However, in several mutant *SOD1* Tg models coexpression of human $SOD1^{WT}$ has been found to exacerbate the disease (Deng et al., 2006, Jaarsma et al., 2000, Prudencio et al., 2010, Wang et al., 2009). Low O_2 tension effects on SOD^{WT} might contribute to the pathology in heterozygous individuals, perhaps through coaggregation of wild-type and mutant SOD1s.

In conclusion, we show that O_2 tension is a principal determinant of SOD1 misfolding and aggregation. Our findings suggest that CNS areas with low O_2 tension could act as foci for the initiation or progression of ALS. This mechanism might contribute to the enhanced risk for the disease associated with aging, as well as other factors that impair vascular perfusion.

Materials and Methods

Human materials

Samples from patients and non-disease controls (Table EV1), including blood samples for genotyping and skin biopsies for fibroblast culture, were collected with approval of the Regional Ethical Review Board in Umeå and in accordance with the principles of the Declaration of Helsinki (WMA, 1964), following written informed consent.

Reagents and chemicals

All reagents and chemicals were obtained from Sigma or Thermo Fisher Scientific unless stated otherwise.

SOD1, FUS, TBK1 and *C9orf72* genotyping

SOD1 and *C9orf72* genotyping were done as described (Keskin et al., 2016). For *FUS,* only exons 2-6 and 11-15 were analyzed. *TBK1* genotyping was performed as described (Freischmidt et al., 2015). All individuals tested negative for mutations in a panel of other ALS-linked genes (details available upon request).

Derivation of human fibroblasts

Following screening of blood to identify *SOD1, FUS, TBK1* and *C9orf72* mutation carriers, fibroblasts were generated from a 3 mm punch skin biopsy (upper arm) from 10 ALS patients with *SOD1* mutations (A4V, H46R, E78_R79insSI, N86S, D90A, G93A, L117V, D125Tfs*24 and G127Gfs*7 (G127X – in 2 patients)). One ALS patient with Q23L mutation in *FUS*, 5 ALS patients with *TBK1* mutations (A417X – in 2 patients, M598V, I450Kfs*14, p.690-713del), 1 ALS and 1 FTD patient with massive intronic GGGGCC repeat-expansions in *C9orf72*, and 4 non-disease control individuals (Table EV1). The establishment of the lines followed standard procedures (Keskin et al., 2016). ALS patients were diagnosed according to EFNS guidelines (Andersen et al., 2005). All patients were heterozygous for their corresponding mutations except the $SOD1^{D90A}$ patient, who was homozygous. Control subjects were relatives of ALS patients. All healthy control subjects tested negative (wt/wt) for a panel of ALS-associated genes including *SOD1, C9orf72, TBK1* and *UBQLN2*.

Generation and maintenance of iPSCs

Fibroblast lines were reprogrammed either with the mRNA Reprogramming Kit (Stemgent, Cambridge, MA, USA) (Warren et al., 2010) using a commercial service (Cellectis AB, Gothenburg, Sweden) or using an episomal vector system (Okita et al., 2011) (Table EV1). IPSCs were cultured using the DEF-CS culture system (Takara Bio Europe, Gothenburg, Sweden) seeded at a density of 40,000 cells/cm^2. Media changes were preformed every 24 h and cells were passaged after 3-4 days at a density of 1.5 - 2x10^5 cells/cm^2 using TrypLE and plated in DEF media supplemented with GF1, GF2 and GF3 (Takara Bio Europe, Gothenburg, Sweden).

Generation of iPSC-MNACs

To generate MNACs, iPSCs at 90% confluence were maintained with N2/B27 media, consisting of DMEM/F12, Neurobasal, 1x Nonessential Amino Acids (NEAA; Millipore, Bedford, MA, USA), 2 mM L-glutamine, 1% (v/v) N2 supplement, 2% (v/v) B27 supplement and penicillin/streptomycin. Over 14 days of differentiation, N2/B27 media were supplemented with 1 μM all-*trans* retinoic acid (RA) and 1 μM smoothened agonist (SAG; Millipore, Bedford, MA, USA). For the first 6 days, cells were kept in N2/B27 media, supplemented with 10 μM SB431542 and 100 nM LDN (Stemgent, Lexington, MA, USA). Dual SMAD inhibition (SB and LDN) was maintained until day 7, after which cells were maintained with N2/B27, supplemented with 4 μM SU5402 (Stemgent, Lexington, MA, USA) and 5 μM DAPT (Selleck Chemicals, Houston, TX, USA) (Lamas et al., 2014).

At Day 14, differentiated cells (neurons and astrocytes) were dissociated to single cells with Accutase and plated onto poly-L-ornithine/laminin-coated 6-well plates (BD Biosciences, Franklin Lakes, NJ, USA) at a density of 100,000 cells/cm^2 or 13 mm diameter coverslips (No. 1.5, VWR, Stockholm, Sweden) at 40,000 cells/cm^2. MNAC cultures were maintained in MN culture media, consisting of Neurobasal, NEAA, 2 mM L-glutamine, 1% (v/v) N2 supplement, 2% (v/v) B27 supplement, 0.4 mg/L ascorbic acid 25 μM glutamate, 25 μM 2-mercaptoethanol, 1 μM RA, 20 μM Y-27632 (Abcam, Cambridge, UK) and penicillin/streptomycin. Cells were incubated in a humidified atmosphere at 37°C supplemented with 5% (v/v) CO_2 and MNAC cultures. On days 11 - 13 days after plating (days 24-26 of the differentiation), MNACs were exposed to different O_2 tensions prior to analysis.

410 **Exposure to different oxygen tensions**

411 Fibroblasts were plated at 8000 cells/cm^2 in 60 mm dishes or 6-well plates (BD Biosciences,
412 Franklin Lakes, NJ, USA) and incubated in an humidified atmosphere at 37°C with 5% (v/v)
413 CO_2. After reaching 60-70% confluence, the medium was replaced prior to exposure to
414 different O_2 tensions. Differentiated MNACs were exposed to different O_2 concentrations
415 without medium change. For O_2 tensions lower than 19%, cells were incubated in a sealed
416 chamber (Biospherix, Lacona, NY, USA) gassed with humidified gas mixtures (1 - 10% O_2,
417 5% CO_2, 94 - 85% N_2) at 37°C. The O_2 concentration was maintained using a ProOx P110
418 oxygen controller (Biospherix, Lacona, NY, USA) supplied with N_2 gas. For each experiment
419 cells were also cultured in parallel under humidified atmospheric O_2 (19% O_2, 5% CO_2, 76%
420 N_2) in a standard tissue culture incubator.
421
422 **Generation of patient-derived primary astrocytes**

423 A piece (2 cm) of ventral horn from the thoracic spinal cord was dissected for cell isolation as
424 previously described (Haidet-Phillips et al., 2011). The tissue was diced and dissociated using
425 2.5 U/ml papain and 0.5 U/ml Dispase (Stemcell Technology, Canada, Inc.) in 1xHBSS
426 supplemented with 40 µg/ml DNAse at 37°C for 45 min with mixing every 5 min Cells were
427 dissociated using a P1000 pipette tip and then mixed with KnockOut DMEM/F12 media
428 containing 10% (v/v) foetal bovine serum (FBS), before filtering the cells through a 0.7 µm
429 cell strainer followed by centrifugation. The cell pellet was resuspended in DMEM/F12 +
430 10% FBS and mixed with an equal volume of Percoll (GE healthcare, Chicago, Illinois). The
431 mixture was centrifuged at 20,000 *g* for 30 min at 4°C and the flocculent layer above the red
432 blood cell layer was collected, washed, resuspended and cultured in primary cell media
433 containing KnockOut DMEM/F12 + 10 % (v/v) FBS supplemented with 20 ng/ml FGF-2, 20
434 ng/ml EGF, 20 ng/ml PDGF-AB (all from Peprotech, Rocky Hill, NJ), 2 mM GlutaMAX
435 Supplement, 1x (v/v) StemPro Neural Supplement and penicillin/streptomycin. The cells were
436 cultured on CELLstart-coated plates and after 24 hours the medium was replaced with serum-
437 free primary cell media. Every 2 days, half of the medium was replaced until cells reached
438 80% confluence after 4-5 weeks. The cells were then passaged, expanded and plated either in
439 coated 6-well plates (BD Biosciences, Franklin Lakes, NJ, USA), for exposure to different O_2
440 tensions, or 13 mm coated coverslips (VWR, Stockholm, Sweden) for immunohistochemistry.
441
442

Cell collection and detergent-insoluble aggregates

Cells were washed at room temperature with PBS containing 40 mM iodoacetamide (IAM), which blocks reduced cysteine residues via alkylation and prevents artificial formation of the C57-C146 disulfide bond (Zetterstrom et al., 2007). The cells were detached with trypsin, and then washed with PBS containing 40 mM IAM and 0.5% (v/v) FBS. After centrifugation of the suspension at 500 *g* for 5 min, the cell pellet was collected and snap frozen on dry ice and stored in a -80°C freezer.

Cell pellets were lysed in ice-cold PBS containing the Complete EDTA-free protease inhibitor cocktail (Roche Diagnostics, Mannheim, Germany), 40 mM IAM and 0.5% (v/v) NP-40 using a Sonifier Cell Disrupter (Branson, Danbury, CT, USA). Lysates were centrifuged at 20,000 *g* for 30 min at 4^{o}C and supernatants were collected and analyzed directly with by misELISA (see below). Pellets were washed twice in ice-cold lysis buffer containing 0.5% (v/v) NP-40 to remove remaining detergent-soluble proteins. The final pellets were used for determination of detergent-insoluble SOD1 aggregates by western blotting.

Immunocapture

A rabbit anti-human SOD1 antibody raised against aa 24-39 of SOD1 was cross-linked to Dynabeads® M-270 Epoxy with the Dynabeads Antibody Coupling Kit (Invitrogen). Beads were recovered with a magnet, washed with the supplied buffers to remove unbound antibody and equilibrated with PBS containing the Complete EDTA-free protease inhibitor cocktail (Roche Diagnostics, Mannheim, Germany), 40 mM IAM and 0.5% (v/v) NP-40. Antibody-coated beads were incubated with 20,000 *g* cell lysate supernatants for 1 h at 23°C. Beads were washed five times with PBS containing the Complete EDTA-free protease inhibitor cocktail (Roche Diagnostics, Mannheim, Germany), 40 mM IAM and 0.5% (v/v) NP-40 and samples were eluted by boiling in 1x sample buffer containing 40 mM IAM. A proportion of the input and non-bound fractions (1/40th), as well as the entire immunocaptured fractions, were analyzed using non-reduced western blotting to determine the proportions of reduced and oxidized SOD1.

Analysis of misfolded and total SOD1 by ELISA

Misfolded SOD1 ELISA (misELISA) was carried out as described (Zetterström et al., 2011, Zetterström et al., 2013). A primary rabbit antibody was raised against a peptide corresponding to aa 24-39 of the human SOD1 sequence. This antibody reacts only with disordered SOD1 species and lacks affinity for the natively folded protein (Bergh et al., 2015, Forsberg et al., 2011, Forsberg et al., 2010). A goat anti-human SOD1 antibody was used as a secondary antibody. It was raised against SOD1 that had been denatured by incubation with guanidinium chloride and EDTA, and reacts preferentially with the disordered protein (Zetterström et al., 2011). For calibration of the misELISA, a fresh spinal cord from a transgenic mouse expressing $hSOD1^{G127X}$ was homogenized in 25 volumes 10 mM K phosphate, pH 7.0 in 0.15 M NaCl, containing the Complete protease inhibitor cocktail (Roche Diagnostics, Mannheim, Germany) and 40 mM IAM. After centrifugation at 20,000 *g*, the supernatant was divided into multiple aliquots that were stored at -80°C. One unit of misfolded SOD1 is defined as the amount present in 1 g wet weight of the original human $SOD1^{G127X}$ standard spinal cord.

The misELISA only reacts with disordered/misfolded SOD1 species. There is no response to holoSOD1 or SOD1s that lack Cu and/or the C57-C146 disulfide bond as long as the polypeptide is natively folded. The cell extracts were incubated for 1 h at 23°C with the capture antibody in the misELISAs. This temperature was selected because at 37°C, some folded SOD1 species have been found to unfold continuously in diluted extracts, such as the cell extracts analyzed here (Zetterström et al., 2013). Moreover, it has been shown that mutations can influence the conformations of immature SOD1 states which could affect the reactivity with the antibodies (Santamaria et al., 2016, Sekhar et al., 2016). Thus, the actual levels of misfolded SOD1 at physiological temperature are not mirrored equally for the SOD1 variants, and misELISA results are not directly comparable between cell lines expressing different SOD1s. However, for a given cell line expressing the same SOD1 variant, the effects of different O_2 tensions on the levels of misfolded SOD1 can be determined.

Total SOD1 was quantified in extracts with a sandwich ELISA based on rabbit capture and goat detection antibodies, both raised against native human SOD1 (Zetterström et al., 2011). It was standardized against human hemolysate with a known SOD1 content calibrated against pure human SOD1, the concentration of which was determined by quantitative amino acid analysis (Marklund et al., 1997).

Western blot, quantification of SOD1 protein, and determination of disulfide-reduced SOD1

The total protein content of cell lysates was determined using the BCA Protein Assay Kit. Western blots were performed in Any kD and 18% (w/v) Criterion TGX precast gels (BioRad Laboratories, Hercules, CA, USA) as previously described (Keskin et al., 2016).

For analysis of SOD1, the primary antibodies used were: rabbit anti-human SOD1 antibodies raised against peptides corresponding to aa 24-39 (2.3 µg/ml), 57–72 (1.6 µg/ml), aa 144-153 (5.2 µg/ml), aa 123-127GQRWK (4.8 µg/ml, G127X-specific) (Jonsson et al., 2006). The same human SOD1 standard described above was used for calibration. For analysis of $SOD1^{G127X}$ using the aa 123-127GQRWK antibody, blots were standardized with an $hSOD1^{G127X}$ transgenic mouse extract in which the $SOD1^{G127X}$ content was determined by western blot using the human-specific aa 24-39 antibody. The proportions of disulfide-reduced and oxidized SOD1 were determined using non-reducing western blotting, i.e. omitting reductant and adding 40 mM IAM to the sample buffer as described (Jonsson et al., 2006, Zetterström et al., 2013, Zetterstrom et al., 2007).

Other antibodies used were rabbit anti-CCS raised against peptides corresponding to aa 252–270 of the human CCS sequence (CCS, 0.9 µg/ml) (Jonsson et al., 2006), rabbit anti-CCS (1:1000 Santa Cruz Biotechnology, Dallas, TX, USA), rabbit anti-glutaredoxin-1 (1:250, Abcam, Cambridge, UK), mouse anti-β-actin (1:200,000; Millipore, Bedford, MA, USA) and rabbit anti-GAPDH (1:1000, Abcam, Cambridge, UK). Secondary antibodies used were horseradish peroxidase (HRP)-conjugated polyclonal anti-mouse or anti-rabbit IgG (1:10,000, Dako, Glostrup, Denmark). ECL Select reagent (GE Healthcare Biosciences, Piscataway, NJ, USA) was used to detect the signal, which was recorded on a ChemiDoc Touch apparatus (BioRad Laboratories, Hercules, CA, USA) and analyzed using ImageLab software (BioRad Laboratories, Hercules, CA, USA).

Effect of cycloheximide on SOD1 misfolding

Fibroblasts were exposed to 19% O_2 or 1% O_2 as described above in the presence and absence of protein synthesis inhibitor CHX (50 µg/ml) for 24 h prior to harvest.

Analysis of reduced and oxidized glutathione

After exposure of MNACs and fibroblasts to different O_2 tensions (1-2-19% O_2) for 24 h as described above, media was aspirated rapidly and 300 µL of ice-cold extraction mixture (0.25 µM glutathione-(glycine-$^{13}C_2$,^{15}N; GSH-IS), 2.5% metaphosphoric acid, 1 mM EDTA and

0.1% formic acid) were added immediately to the cells. After scraping, the resulting cell suspensions were snap-frozen and stored at -80°C until analysis.

For analysis, a tungsten bead was added to the tubes, which were then homogenized in a bead mill (Retsch MM400) at 30 oscillations/s for 1 min, followed by centrifugation at 22,000 *g* for 20 min Fifty µL of the resulting supernatant was transferred to a LC-MS vial and 1 µL was injected and analyzed by LC-ESI-MSMS (1290 Infinity system from Agilent Technologies, with an Acquity UPLC HSS T3 column, thermostatted to 40°C and coupled to an Agilent 6490 Triple quadrupole mass spectrometer). The analysis was performed as essentially as described (Cao et al., 2013) by comparison to GSH and GSSG solutions made in water (2.5 mM metaphosphoric acid, 1 mM EDTA, 0.1% formic acid) at twelve different calibration concentrations (0.01-10 µM) and containing the GSH-IS.

GSH and GSSG concentrations were normalized to the protein content of the corresponding 22,000 *g* pellets after extraction. Pellets were resuspended by sonication/boiling in sample buffer. Protein estimation was performed using the BCA Protein Assay Kit and bovine serum albumin standards boiled in 1x sample buffer.

Immunocytochemistry

Cells were fixed in 3.8% (w/v) formaldehyde for 10 min at room temperature, and blocked with 10% (v/v) FBS in PBS containing 0.1% (v/v) Triton X-100 for 1 h at room temperature. Cells were incubated with primary antibodies overnight at 4°C. The primary antibodies used were; anti-neuron-specific class III beta-tubulin (TUBB3, TUJ1, 1:7500, Covance Inc. Princeton, NJ, USA), microtubule-associated protein 2 (MAP2; 1:500, Millipore, Bedford, MA, USA), SMI32 (1:1000, Covance Inc. Princeton, NJ, USA), ISL1/2 (39.4D5,1:5, developed by T.M. Jessell and S. Brenner-Morton, Developmental Studies Hybridoma Bank, created by the NICHD of the NIH and maintained at The University of Iowa, Department of Biology, Iowa City, IA, USA), S100β (1:200) and vimentin (1:1000 Progen, Heidelberg, Germany). Next day, the coverslips were washed and incubated with Alexa-Fluor conjugated secondary antibodies (1:1000) for 1 h at room temperature, and nuclei were counterstained with 4',6-diamidino-2-phenylindole (DAPI; 0.3 µM). Cells were mounted in Aqua-Polymount (Polysciences, Inc., Warrington, PA, USA).

In vitro cell cytotoxicity assays

Dead cells that had lost plasma membrane integrity were quantified using the luminogenic substrate AAF-Glo (CytoTox-Glo Cell Viability Assay, Promega, Madison, WI, USA) as previously described (Keskin et al., 2016). Cell viability was calculated by subtracting the luminescence signal obtained before, from the total luminescence values obtained after, permeabilization with digitonin according to the manufacturer's protocol.

Cellular ATP content was determined using the CellTiter-Glo Luminescent Cell Viability Assay (Promega, Madison, WI, USA).

Proteasome activity assay

A cell-based luminescent proteasome assay (Proteasome-Glo, Promega, Madison, WI, USA) was used to measure chymotrypsin-like proteasome activity as described (Keskin et al., 2016). The assay contains the luminogenic peptide substrate Suc-LLVY-aminoluciferin for determination of chymotrypsin-like activity of the proteasome.

Statistical analyses

Statistical analyses were performed using GraphPad Prism version 6.00 (La Jolla, CA, USA). To test for statistical significance between two groups, the Mann-Whitney U test was used. For statistical significance testing between multiple groups, the Kruskal-Wallis test followed by Dunn's post hoc test was used. The significance level was set to 0.05. All values are given as means ± SD.

Acknowledgements

We thank the many individuals that generously provided patient or control samples. We thank Anna Wuolikainen for valuable discussions and Agneta Öberg, Eva Jonsson, Eva Bern, and Matthew Marklund for skillful technical assistance. The study was supported by the Swedish Research Council (VRMH 2015-02804), the Knut and Alice Wallenberg Foundation (2012.0091), the Bertil Hållsten Foundation, the Torsten Söderberg Foundation, the Swedish Brain Fund (Hjärnfonden FO2015-0234), the Ulla-Carin Lindquist Foundation, Neuroförbundet, the Stratneuro Initiative, Västerbotten County Council, and the Kempe Foundations. MS was supported by the Else Kröner Fresenius Stiftung.

Author contributions

Conception and design of the work: IK, EF, ML, UN, PMA, PZ, SLM, JDG. Clinical and pathological diagnoses and sample collection: DJL, MS, TB, PMA. Acquisition, analysis, or interpretation of the data: IK, EF, ML, PMA, TB, UN, PZ, SLM, JDG. Drafting or revising the manuscript for intellectual content: IK, EF, ML, UN, PMA, SLM, JDG with input from all authors. Final approval of the manuscript: All authors.

Conflict of interest

The authors declare that they have no conflict of interest.

Figure legends

Figure 1. Experimental overview and generation of mixed motor neuron and astrocyte cultures (MNACs) derived from induced pluripotent stem cells (iPSCs).

(A) Patient-derived fibroblasts, primary spinal cord ventral horn astrocytes and iPSC-derived MNACs were exposed to different O_2 tensions for 24 h prior to analysis. (B) Patient-derived fibroblasts were reprogrammed to iPSCs using the 4 Yamanaka factors and then differentiated to a forelimb level, ventral spinal cord identity over 14 days. At Day 14, differentiated cells were dissociated and plated on poly-L-ornithine/laminin and matured for 10 more days. MNACs were used for O_2 tension experiments at Day 25.

Figure 2. Concentration- and time-dependent misfolding of SOD1 in response to low oxygen tensions.

Misfolded SOD1 quantified in fibroblast extracts by misELISA, normalized to total protein and presented as a ratio to the level present in replicate cultures maintained at 19% O_2 for 24 h. (A) O_2 concentration- (19-1%) and (B) time- (1-24 h) dependent increases in misfolded SOD1 in fibroblast lines. Data are expressed as the mean ± SD (n = 3 replicate culture wells). (C) Reversal of the misfolding response following transfer of cultures from 1% O_2/24 h to 19% O_2. Data are expressed as the mean ± SD (n = 3 replicate culture wells for Control and $SOD1^{G127X}$, 2 replicate experiments each with 3 replicate cultures for G93A), $*p < 0.05$ analyzed by the Kruskal-Wallis test followed by Dunn's test. (D) Misfolding response in patient-derived fibroblast lines and (E) primary astrocytes following exposure to 1% O_2 for 24 h. Data are expressed as the mean ± SD (n = 3 to 15; 1-5 replicate experiments each with 3 replicate cultures), $*p < 0.05$, $**p < 0.01$, $****p < 0.0001$ analyzed by Mann-Whitney U test. Blue bars = fibroblasts, green bars = astrocytes, grey bars = corresponding cell lines cultured at 19% O_2.

Figure 3. Enhanced misfolding response in patient-derived MNACs.

Misfolded SOD1 quantified in MNAC extracts by misELISA, normalized to total protein and presented as a ratio to the level present in replicate cultures maintained at 19% O_2 for 24 h. (A) O_2 tension (19-2%) dependent increases in misfolded SOD1. Data are expressed as the mean ± SD (n = 6; 2 replicate experiments from independent differentiations, each with 3 replicate cultures), $*p < 0.05$, $**p < 0.01$, $****p < 0.0001$, analyzed by Kruskal-Wallis test

followed by Dunn's test. (B) SOD1 misfolding is increased in MNACs following exposure to 2% O_2 for 24 h. Data are expressed as the mean ± SD (n = 6 to 18; 2-6 replicate experiments from independent differentiations, each with 3 replicate cultures), *$p < 0.05$, **$p < 0.01$, ****$p < 0.0001$, analyzed by Mann-Whitney U test.

Figure 4. Low O_2 tension promotes disulfide bond reduction and misfolding of SOD1.

Analysis of MNAC extracts following exposure to 19% or 2% O_2 for 24 h. (A) Disulfide-reduced (red) and -oxidized (ox) SOD1 were resolved by non-reducing SDS-PAGE followed by western blotting with an anti-SOD1 24-39 aa antibody. (B) Scatter plot showing the ratios of disulfide-reduced to -oxidized SOD1 at 19% (grey circles) O_2 versus 2% (red circles). Data are expressed as the mean ± SD (n = 4 to 8; 2-6 replicate experiments from independent differentiations, each with 3 replicate cultures), *$p < 0.05$, **$p < 0.01$, ***$p < 0.001$, analyzed by the Mann-Whitney U test to compare to the respective line cultured at 19% O_2 for 24 h. (C) Western blot showing analysis of immunocaptured misfolded SOD1. Input (I, $1/40^{th}$ of the sample), non-bound (NB, $1/40^{th}$) and immunocaptured (IC, entire sample) fractions of SOD1 from MNACs cultured at 19% O_2 or 2% O_2 for 24 h using anti-SOD1 24-39 aa. Disulfide-reduced and -oxidized SOD1 were quantified using anti-SOD1 aa 57-72. Only disulfide-reduced SOD1 was captured.

Figure 5. Low O_2 tension does not alter known determinants of SOD1 C57-C146 redox status.

(A) CCS and (B) glutaredoxin-1 quantified in MNAC extracts by western blotting and normalized to β-actin as a loading control. Cells exposed to 19% O_2 (grey bars) or 2% O_2 (red bars) for 24 h. Plotted as a ratio of the level present in replicate cultures maintained at 19% O_2 for 24 h. Data are expressed as the mean ± SD (n = 4 to 10; 2-6 replicate experiments from independent differentiations, each with 3 replicate cultures), analyzed by Mann-Whitney U test. (C) GSH levels, (D) GSSG levels and (E) GSH/GSSG ratios determined in MNACs (left, red bars) and fibroblasts (right, blue bars). Data are expressed as the mean ± SD (n = 6; 2 replicate experiments from independent differentiations, each with 3 replicates for MNACs) and (n = 3 replicate cultures of fibroblasts), *$p < 0.05$, analyzed by the Mann-Whitney U test to compare to the respective line cultured at 19% O_2 for 24 h.

Figure 6. Low O_2 tension increases disulfide bond reduction in both nascent and mature SOD1.

Misfolded SOD1 quantified in; (A) Control I, (B) $SOD1^{G127X}$ and (C) $SOD1^{G93A}$ fibroblast extracts by misELISA, normalized to total protein. Cells grown at 19% O_2 (grey bars) or 1% O_2 (blue bars) for 24 h in the absence, or presence (checker board pattern), of cycloheximide (CHX; 50 µg/ml). Data are expressed as the mean ± SD (n = 3 replicate cultures for Control I and $SOD1^{G127X}$) and (n = 6; 2 replicate experiments each with 3 replicate cultures for $SOD1^{G93A}$ normalized by division by the means of each experiment), $^{**}p < 0.01$, analyzed by the Mann-Whitney U-test.

Figure 7. Low O_2 tension promotes SOD1 aggregation in MNACs but not in fibroblasts.

Scatter plots show the amounts of SOD1 present in the detergent-insoluble fraction determined by western blotting as a % of soluble SOD1 present in the cell extract determined by ELISA; MNACs (red; 2% O_2/24 h) and fibroblasts (blue; 1% O_2/24 h) in comparison to replicate cultures (grey; 19% O_2/24 h). Full-length SOD1s are depicted as filled circles. The aa 57-72 antibody used for detection showed relatively strong bands in the $SOD1^{D125Tfs*24}$ samples (Fig EV6A). This represents mutant SOD1 (filled squares), since negligible bands were detected using an antibody raised against a C-terminal SOD1 (aa 143-153) peptide (Fig EV6E). The $SOD1^{G127X}$ mutant protein (filled triangles) was quantified using a $hSOD1^{G127X}$-specific antibody (Fig EV6 B and D). Data are expressed as the means ± SD (n = 4 to 10; 2-6 replicate experiments from independent differentiations, each with 3 replicates for MNACs) and (n = 3 to 6; 1-3 experiments each with 3 replicates for fibroblasts), $^{*}p < 0.05$, $^{**}p < 0.01$, $^{***}p < 0.001$, analyzed by the Mann-Whitney U test.

References

733 Alavi A, Nafissi S, Rohani M, Zamani B, Sedighi B, Shamshiri H, Fan JB, Ronaghi M, Elahi E (2013)
734 Genetic analysis and SOD1 mutation screening in Iranian amyotrophic lateral sclerosis patients.
735 Neurobiology of aging 34: 1516 e1-8
736 Amoroso MW, Croft GF, Williams DJ, O'Keeffe S, Carrasco MA, Davis AR, Roybon L, Oakley DH,
737 Maniatis T, Henderson CE, Wichterle H (2013) Accelerated high-yield generation of limb-
738 innervating motor neurons from human stem cells. The Journal of neuroscience : the official
739 journal of the Society for Neuroscience 33: 574-86
740 Andersen PM, Al-Chalabi A (2011) Clinical genetics of amyotrophic lateral sclerosis: what do we
741 really know? Nature reviews Neurology 7: 603-15
742 Andersen PM, Borasio GD, Dengler R, Hardiman O, Kollewe K, Leigh PN, Pradat PF, Silani V,
743 Tomik B (2005) EFNS task force on management of amyotrophic lateral sclerosis: guidelines for
744 diagnosing and clinical care of patients and relatives. European journal of neurology : the official
745 journal of the European Federation of Neurological Societies 12: 921-38
746 Andersen PM, Forsgren L, Binzer M, Nilsson P, Ala-Hurula V, Keranen ML, Bergmark L, Saarinen
747 A, Haltia T, Tarvainen I, Kinnunen E, Udd B, Marklund SL (1996) Autosomal recessive adult-
748 onset amyotrophic lateral sclerosis associated with homozygosity for Asp90Ala CuZn-superoxide
749 dismutase mutation. A clinical and genealogical study of 36 patients. Brain : a journal of neurology
750 119 (Pt 4): 1153-72
751 Andersen PM, Nilsson P, Ala-Hurula V, Keränen ML, Tarvainen I, Haltia T, Nilsson L, Binzer M,
752 Forsgren L, Marklund SL (1995) Amyotrophic lateral sclerosis associated with homozygosity for
753 an Asp90Ala mutation in CuZn-superoxide dismutase. Nat Genet 10: 61-6
754 Ayers JI, Fromholt S, Koch M, DeBosier A, McMahon B, Xu G, Borchelt DR (2014) Experimental
755 transmissibility of mutant SOD1 motor neuron disease. Acta Neuropathol 128: 791-803
756 Ayers JI, Fromholt SE, O'Neal VM, Diamond JH, Borchelt DR (2016) Prion-like propagation of
757 mutant SOD1 misfolding and motor neuron disease spread along neuroanatomical pathways. Acta
758 Neuropathol 131: 103-14
759 Bergemalm D, Forsberg K, Srivastava V, Graffmo KS, Andersen PM, Brannstrom T, Wingsle G,
760 Marklund SL (2010) Superoxide dismutase-1 and other proteins in inclusions from transgenic
761 amyotrophic lateral sclerosis model mice. J Neurochem 114: 408-18
762 Bergh J, Zetterström P, Andersen PM, Brännström T, Graffmo KS, Jonsson PA, Lang L, Danielsson J,
763 Oliveberg M, Marklund SL (2015) Structural and kinetic analysis of protein-aggregate strains in
764 vivo using binary epitope mapping. Proc Natl Acad Sci U S A 112: 4489-94
765 Bidhendi EE, Bergh J, Zetterstrom P, Andersen PM, Marklund SL, Brannstrom T (2016) Two
766 superoxide dismutase prion strains transmit amyotrophic lateral sclerosis-like disease. J Clin Invest
767 126: 2249-53
768 Birve A, Neuwirth C, Weber M, Marklund SL, Nilsson AC, Jonsson PA, Andersen PM (2010) A
769 novel SOD1 splice site mutation associated with familial ALS revealed by SOD activity analysis.
770 Human molecular genetics 19: 4201-6
771 Bordo D, Djinovic K, Bolognesi M (1994) Conserved patterns in the Cu,Zn superoxide dismutase
772 family. Journal of molecular biology 238: 366-86
773 Bosco DA, Morfini G, Karabacak NM, Song Y, Gros-Louis F, Pasinelli P, Goolsby H, Fontaine BA,
774 Lemay N, McKenna-Yasek D, Frosch MP, Agar JN, Julien JP, Brady ST, Brown RH, Jr. (2010)
775 Wild-type and mutant SOD1 share an aberrant conformation and a common pathogenic pathway in
776 ALS. Nat Neurosci 13: 1396-403
777 Boukaftane Y, Khoris J, Moulard B, Salachas F, Meininger V, Malafosse A, Camu W, Rouleau GA
778 (1998) Identification of six novel SOD1 gene mutations in familial amyotrophic lateral sclerosis.
779 Can J Neurol Sci 25: 192-6
780 Cao L, Waldon D, Teffera Y, Roberts J, Wells M, Langley M, Zhao Z (2013) Ratios of biliary
781 glutathione disulfide (GSSG) to glutathione (GSH): a potential index to screen drug-induced
782 hepatic oxidative stress in rats and mice. Anal Bioanal Chem 405: 2635-42
783 Carroll MC, Outten CE, Proescher JB, Rosenfeld L, Watson WH, Whitson LJ, Hart PJ, Jensen LT,
784 Cizewski Culotta V (2006) The effects of glutaredoxin and copper activation pathways on the
785 disulfide and stability of Cu,Zn superoxide dismutase. The Journal of biological chemistry 281:
786 28648-56

787 Charcot JM (1873) Lecons sur les maladies du système nervaux. 2nd series, collected by Bourneville.
788 Charcot, J.M. (1881) Lectures on the diseases of the nervous system, Vol 2, series 2, Sigersen G
789 (trans and ed). London: New Sydenham Society, 163-204.
790 Chattopadhyay M, Durazo A, Sohn SH, Strong CD, Gralla EB, Whitelegge JP, Valentine JS (2008)
791 Initiation and elongation in fibrillation of ALS-linked superoxide dismutase. Proc Natl Acad Sci U
792 S A 105: 18663-8
793 Chattopadhyay M, Nwadibia E, Strong CD, Gralla EB, Valentine JS, Whitelegge JP (2015) The
794 Disulfide Bond, but Not Zinc or Dimerization, Controls Initiation and Seeded Growth in
795 Amyotrophic Lateral Sclerosis-linked Cu,Zn Superoxide Dismutase (SOD1) Fibrillation. The
796 Journal of biological chemistry 290: 30624-36
797 Chio A, Benzi G, Dossena M, Mutani R, Mora G (2005) Severely increased risk of amyotrophic
798 lateral sclerosis among Italian professional football players. Brain : a journal of neurology 128:
799 472-6
800 Culotta VC, Klomp LW, Strain J, Casareno RL, Krems B, Gitlin JD (1997) The copper chaperone for
801 superoxide dismutase. J Biol Chem 272: 23469-72
802 Da Cruz S, Bui A, Saberi S, Lee SK, Stauffer J, McAlonis-Downes M, Schulte D, Pizzo DP, Parone
803 PA, Cleveland DW, Ravits J (2017) Misfolded SOD1 is not a primary component of sporadic ALS.
804 Acta neuropathologica 134: 97-111
805 Deng HX, Shi Y, Furukawa Y, Zhai H, Fu R, Liu E, Gorrie GH, Khan MS, Hung WY, Bigio EH,
806 Lukas T, Dal Canto MC, O'Halloran TV, Siddique T (2006) Conversion to the amyotrophic lateral
807 sclerosis phenotype is associated with intermolecular linked insoluble aggregates of SOD1 in
808 mitochondria. Proceedings of the National Academy of Sciences of the United States of America
809 103: 7142-7
810 Erecinska M, Silver IA (2001) Tissue oxygen tension and brain sensitivity to hypoxia. Respiration
811 physiology 128: 263-76
812 Fetherolf MM, Boyd SD, Taylor AB, Kim HJ, Wohlschlegel JA, Blackburn NJ, Hart PJ, Winge DR,
813 Winkler DD (2017) Copper-zinc superoxide dismutase is activated through a sulfenic acid
814 intermediate at a copper-ion entry site. The Journal of biological chemistry
815 Forsberg K, Andersen PM, Marklund SL, Brännström T (2011) Glial nuclear aggregates of superoxide
816 dismutase-1 are regularly present in patients with amyotrophic lateral sclerosis. Acta Neuropathol
817 121: 623-34
818 Forsberg K, Jonsson PA, Andersen PM, Bergemalm D, Graffmo KS, Hultdin M, Jacobsson J,
819 Rosquist R, Marklund SL, Brännström T (2010) Novel antibodies reveal inclusions containing non-
820 native SOD1 in sporadic ALS patients. PLoS One 5: e11552
821 Forsgren E, Lehmann M, Mathis MW, Keskin I, Zetterström P, Nijssen J, Lowry ER, Garcia A,
822 Sandoe J, Hedlund E, Wichterle H, Henderson C, Eggan K, Kiskinis E, Andersen PM, Marklund
823 SL, Gilthorpe JD (under revision) Enhanced protein misfolding in patient-derived models of
824 amyotrophic lateral sclerosis. Stem Cell Reports
825 Freischmidt A, Wieland T, Richter B, Ruf W, Schaeffer V, Muller K, Marroquin N, Nordin F, Hubers
826 A, Weydt P, Pinto S, Press R, Millecamps S, Molko N, Bernard E, Desnuelle C, Soriani MH, Dorst
827 J, Graf E, Nordstrom U et al. (2015) Haploinsufficiency of TBK1 causes familial ALS and fronto-
828 temporal dementia. Nature neuroscience 18: 631-6
829 Furukawa Y, Kaneko K, Yamanaka K, O'Halloran TV, Nukina N (2008) Complete loss of post-
830 translational modifications triggers fibrillar aggregation of SOD1 in the familial form of
831 amyotrophic lateral sclerosis. J Biol Chem 283: 24167-76
832 Furukawa Y, Torres AS, O'Halloran TV (2004) Oxygen-induced maturation of SOD1: a key role for
833 disulfide formation by the copper chaperone CCS. EMBO J 23: 2872-81
834 Gallo V, Bueno-De-Mesquita HB, Vermeulen R, Andersen PM, Kyrozis A, Linseisen J, Kaaks R,
835 Allen NE, Roddam AW, Boshuizen HC, Peeters PH, Palli D, Mattiello A, Sieri S, Tumino R,
836 Jimenez-Martin JM, Diaz MJ, Suarez LR, Trichopoulou A, Agudo A et al. (2009) Smoking and
837 risk for amyotrophic lateral sclerosis: analysis of the EPIC cohort. Annals of neurology 65: 378-85
838 Gallo V, Vanacore N, Bueno-de-Mesquita HB, Vermeulen R, Brayne C, Pearce N, Wark PA, Ward
839 HA, Ferrari P, Jenab M, Andersen PM, Wennberg P, Wareham N, Katzke V, Kaaks R, Weiderpass
840 E, Peeters PH, Mattiello A, Pala V, Barricante A et al. (2016) Physical activity and risk of

Amyotrophic Lateral Sclerosis in a prospective cohort study. European journal of epidemiology 31: 255-66

Graffmo KS, Forsberg K, Bergh J, Birve A, Zetterstrom P, Andersen PM, Marklund SL, Brannstrom T (2013) Expression of wild-type human superoxide dismutase-1 in mice causes amyotrophic lateral sclerosis. Hum Mol Genet 22: 51-60

Haidet-Phillips AM, Hester ME, Miranda CJ, Meyer K, Braun L, Frakes A, Song S, Likhite S, Murtha MJ, Foust KD, Rao M, Eagle A, Kammesheidt A, Christensen A, Mendell JR, Burghes AHM, Kaspar BK (2011) Astrocytes from familial and sporadic ALS patients are toxic to motor neurons. Nat Biotechnol 29: 824-8

Hayward C, Brock DJ, Minns RA, Swingler RJ (1998) Homozygosity for Asn86Ser mutation in the CuZn-superoxide dismutase gene produces a severe clinical phenotype in a juvenile onset case of familial amyotrophic lateral sclerosis. Journal of medical genetics 35: 174

Iadecola C (2017) The Neurovascular Unit Coming of Age: A Journey through Neurovascular Coupling in Health and Disease. Neuron 96: 17-42

Jaarsma D, Haasdijk ED, Grashorn JA, Hawkins R, van Duijn W, Verspaget HW, London J, Holstege JC (2000) Human Cu/Zn superoxide dismutase (SOD1) overexpression in mice causes mitochondrial vacuolization, axonal degeneration, and premature motoneuron death and accelerates motoneuron disease in mice expressing a familial amyotrophic lateral sclerosis mutant SOD1. Neurobiology of disease 7: 623-43

Jonsson PA, Ernhill K, Andersen PM, Bergemalm D, Brännström T, Gredal O, Nilsson P, Marklund SL (2004) Minute quantities of misfolded mutant superoxide dismutase-1 cause amyotrophic lateral sclerosis. Brain 127: 73-88

Jonsson PA, Graffmo KS, Andersen PM, Brännström T, Lindberg M, Oliveberg M, Marklund SL (2006) Disulphide-reduced superoxide dismutase-1 in CNS of transgenic amyotrophic lateral sclerosis models. Brain 129: 451-64

Karch CM, Prudencio M, Winkler DD, Hart PJ, Borchelt DR (2009) Role of mutant SOD1 disulfide oxidation and aggregation in the pathogenesis of familial ALS. Proc Natl Acad Sci U S A 106: 7774-9

Kato M, Aoki M, Ohta M, Nagai M, Ishizaki F, Nakamura S, Itoyama Y (2001) Marked reduction of the Cu/Zn superoxide dismutase polypeptide in a case of familial amyotrophic lateral sclerosis with the homozygous mutation. Neurosci Lett 312: 165-8

Kato S, Takikawa M, Nakashima K, Hirano A, Cleveland DW, Kusaka H, Shibata N, Kato M, Nakano I, Ohama E (2000) New consensus research on neuropathological aspects of familial amyotrophic lateral sclerosis with superoxide dismutase 1 (SOD1) gene mutations: inclusions containing SOD1 in neurons and astrocytes. Amyotroph Lateral Scler Other Motor Neuron Disord 1: 163-84

Keskin I, Birve A, Berdynski M, Hjertkvist K, Rofougaran R, Nilsson TK, Glass JD, Marklund SL, Andersen PM (2017) Comprehensive analysis to explain reduced or increased SOD1 enzymatic activity in ALS patients and their relatives. Amyotrophic lateral sclerosis & frontotemporal degeneration 18: 457-463

Keskin I, Forsgren E, Lange DJ, Weber M, Birve A, Synofzik M, Gilthorpe JD, Andersen PM, Marklund SL (2016) Effects of Cellular Pathway Disturbances on Misfolded Superoxide Dismutase-1 in Fibroblasts Derived from ALS Patients. PLoS One 11: e0150133

Lamas NJ, Johnson-Kerner B, Roybon L, Kim YA, Garcia-Diaz A, Wichterle H, Henderson CE (2014) Neurotrophic requirements of human motor neurons defined using amplified and purified stem cell-derived cultures. PLoS One 9: e110324

Lang L, Kurnik M, Danielsson J, Oliveberg M (2012) Fibrillation precursor of superoxide dismutase 1 revealed by gradual tuning of the protein-folding equilibrium. Proc Natl Acad Sci U S A 109: 17868-73

Lyons DG, Parpaleix A, Roche M, Charpak S (2016) Mapping oxygen concentration in the awake mouse brain. eLife 5

Marklund SL, Andersen PM, Forsgren L, Nilsson P, Ohlsson PI, Wikander G, Oberg A (1997) Normal binding and reactivity of copper in mutant superoxide dismutase isolated from amyotrophic lateral sclerosis patients. J Neurochem 69: 675-81

Mercatelli E, Barbieri L, Luchinat E, Banci L (2016) Direct structural evidence of protein redox regulation obtained by in-cell NMR. Biochimica et biophysica acta 1863: 198-204

Miller AF (2012) Superoxide dismutases: ancient enzymes and new insights. FEBS letters 586: 585-95

Okita K, Matsumura Y, Sato Y, Okada A, Morizane A, Okamoto S, Hong H, Nakagawa M, Tanabe K, Tezuka K, Shibata T, Kunisada T, Takahashi M, Takahashi J, Saji H, Yamanaka S (2011) A more efficient method to generate integration-free human iPS cells. Nature methods 8: 409-12

Pettersen EO, Larsen LH, Ramsing NB, Ebbesen P (2005) Pericellular oxygen depletion during ordinary tissue culturing, measured with oxygen microsensors. Cell proliferation 38: 257-67

Pokrishevsky E, Grad LI, Yousefi M, Wang J, Mackenzie IR, Cashman NR (2012) Aberrant localization of FUS and TDP43 is associated with misfolding of SOD1 in amyotrophic lateral sclerosis. PloS one 7: e35050

Prudencio M, Durazo A, Whitelegge JP, Borchelt DR (2010) An examination of wild-type SOD1 in modulating the toxicity and aggregation of ALS-associated mutant SOD1. Human molecular genetics 19: 4774-89

Prudencio M, Hart PJ, Borchelt DR, Andersen PM (2009) Variation in aggregation propensities among ALS-associated variants of SOD1: correlation to human disease. Hum Mol Genet 18: 3217-26

Rosen DR, Siddique T, Patterson D, Figlewicz DA, Sapp P, Hentati A, Donaldson D, Goto J, O'Regan JP, Deng HX, et al. (1993) Mutations in Cu/Zn superoxide dismutase gene are associated with familial amyotrophic lateral sclerosis. Nature 362: 59-62

Rosenbohm A, Kassubek J, Weydt P, Marroquin N, Volk AE, Kubisch C, Huppertz HJ, Weber M, Andersen PM, Weishaupt JH, Ludolph AC, Group ALSSR (2014) Can lesions to the motor cortex induce amyotrophic lateral sclerosis? Journal of neurology 261: 283-90

Santamaria N, Alhothali M, Alfonso MH, Breydo L, Uversky VN (2016) Intrinsic disorder in proteins involved in amyotrophic lateral sclerosis. Cell Mol Life Sci

Sato T, Nakanishi T, Yamamoto Y, Andersen PM, Ogawa Y, Fukada K, Zhou Z, Aoike F, Sugai F, Nagano S, Hirata S, Ogawa M, Nakano R, Ohi T, Kato T, Nakagawa M, Hamasaki T, Shimizu A, Sakoda S (2005) Rapid disease progression correlates with instability of mutant SOD1 in familial ALS. Neurology 65: 1954-7

Schwarzlander M, Dick TP, Meyer AJ, Morgan B (2016) Dissecting Redox Biology Using Fluorescent Protein Sensors. Antioxidants & redox signaling 24: 680-712

Sekhar A, Rumfeldt JA, Broom HR, Doyle CM, Sobering RE, Meiering EM, Kay LE (2016) Probing the free energy landscapes of ALS disease mutants of SOD1 by NMR spectroscopy. Proc Natl Acad Sci U S A

Synofzik M, Ronchi D, Keskin I, Basak AN, Wilhelm C, Gobbi C, Birve A, Biskup S, Zecca C, Fernández-Santiago R, Kaugesaar T, Schöls L, Marklund SL, Andersen PM (2012) Mutant superoxide dismutase-1 indistinguishable from wild-type causes ALS. Hum Mol Genet 21: 3568-74

Turner MR, Goldacre R, Talbot K, Goldacre MJ (2016) Cerebrovascular injury as a risk factor for amyotrophic lateral sclerosis. Journal of neurology, neurosurgery, and psychiatry 87: 244-6

Wang L, Deng HX, Grisotti G, Zhai H, Siddique T, Roos RP (2009) Wild-type SOD1 overexpression accelerates disease onset of a G85R SOD1 mouse. Human molecular genetics 18: 1642-51

Warren L, Manos PD, Ahfeldt T, Loh YH, Li H, Lau F, Ebina W, Mandal PK, Smith ZD, Meissner A, Daley GQ, Brack AS, Collins JJ, Cowan C, Schlaeger TM, Rossi DJ (2010) Highly efficient reprogramming to pluripotency and directed differentiation of human cells with synthetic modified mRNA. Cell Stem Cell 7: 618-30

Winkler DD, Schuermann JP, Cao X, Holloway SP, Borchelt DR, Carroll MC, Proescher JB, Culotta VC, Hart PJ (2009) Structural and biophysical properties of the pathogenic SOD1 variant H46R/H48Q. Biochemistry 48: 3436-47

Zetterström P, Andersen PM, Brännström T, Marklund SL (2011) Misfolded superoxide dismutase-1 in CSF from amyotrophic lateral sclerosis patients. J Neurochem 117: 91-9

Zetterström P, Graffmo KS, Andersen PM, Brännström T, Marklund SL (2013) Composition of soluble misfolded superoxide dismutase-1 in murine models of amyotrophic lateral sclerosis. Neuromolecular Med 15: 147-58

Zetterstrom P, Stewart HG, Bergemalm D, Jonsson PA, Graffmo KS, Andersen PM, Brannstrom T, Oliveberg M, Marklund SL (2007) Soluble misfolded subfractions of mutant superoxide dismutase-

1s are enriched in spinal cords throughout life in murine ALS models. Proc Natl Acad Sci U S A 104: 14157-62

Figure 1

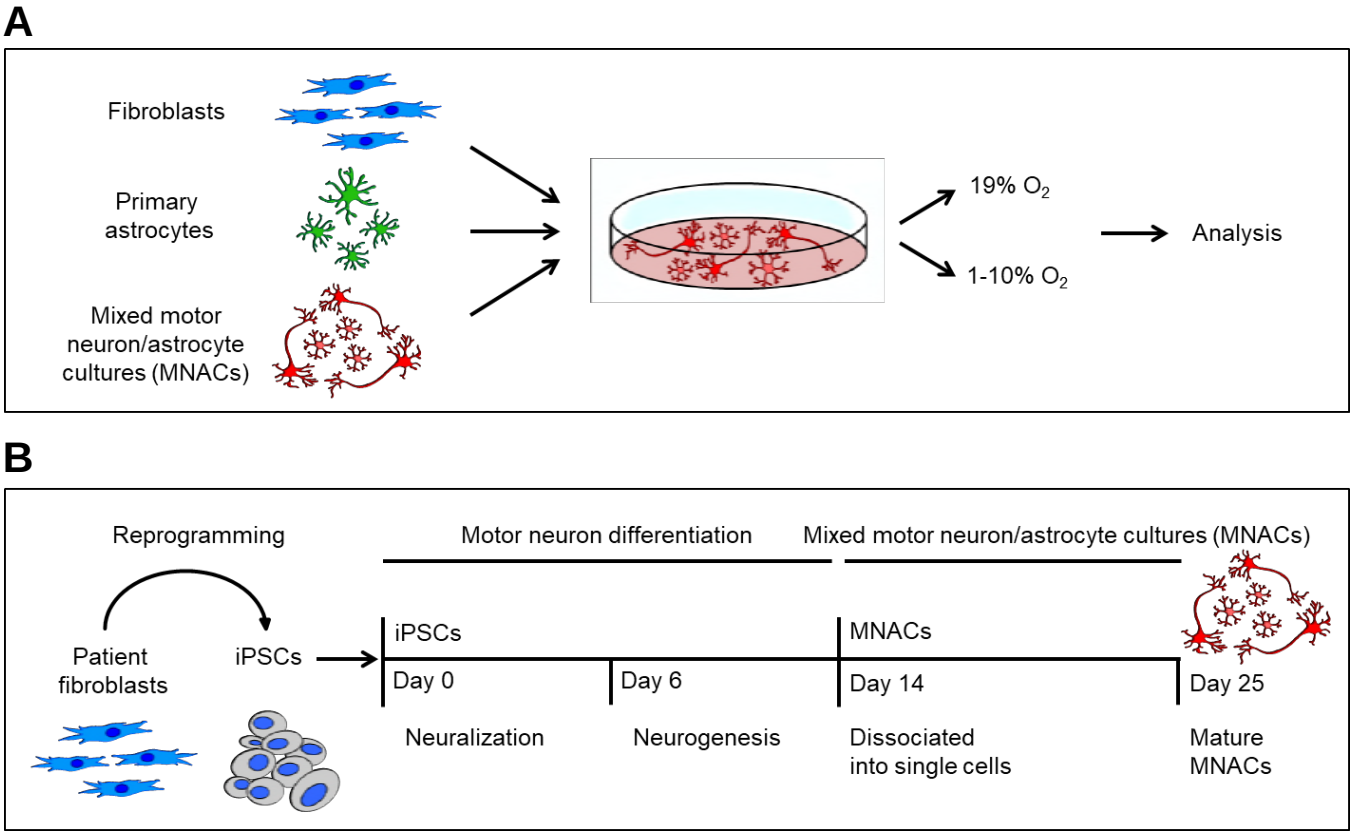
A
Fibroblasts
Primary astrocytes
Mixed motor neuron/astrocyte cultures (MNACs)
19% O_2
1-10% O_2
Analysis
B
Reprogramming
Motor neuron differentiation
Mixed motor neuron/astrocyte cultures (MNACs)
Patient fibroblasts
iPSCs
iPSCs
MNACs
Day 0
Day 6
Day 14
Day 25
Neuralization
Neurogenesis
Dissociated into single cells
Mature MNACs

Figure 2

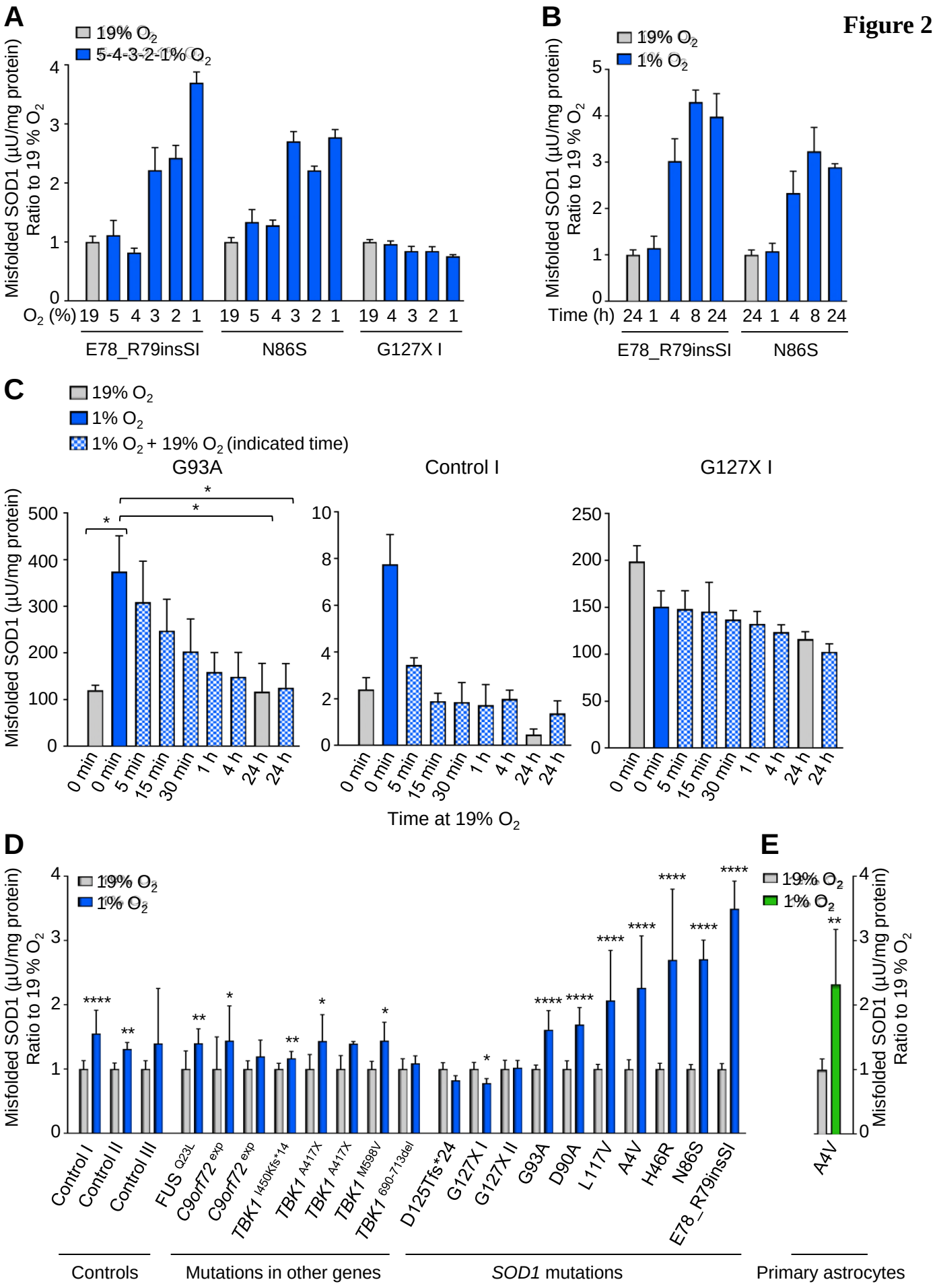
A
19% O2
5-4-3-2-1% O2
Misfolded SOD1 (µU/mg protein)
Ratio to 19 % O2
O2 (%) 19 5 4 3 2 1 19 5 4 3 2 1 19 4 3 2 1
E78_R79insSI
N86S
G127X I
B
19% O2
1% O2
Misfolded SOD1 (µU/mg protein)
Ratio to 19 % O2
Time (h) 24 1 4 8 24 24 1 4 8 24
E78_R79insSI
N86S
C
19% O2
1% O2
1% O2 + 19% O2 (indicated time)
G93A
Control I
G127X I
Misfolded SOD1 (µU/mg protein)
0 min 0 min 5 min 15 min 30 min 1 h 4 h 24 h 24 h
Time at 19% O2
D
19% O2
1% O2
Misfolded SOD1 (µU/mg protein)
Ratio to 19 % O2
Control I
Control II
Control III
FUS Q23L
C9orf72 exp
C9orf72 exp
TBK1 I450Kfs*14
TBK1 A417X
TBK1 A417X
TBK1 M598V
TBK1 690-713del
D125Tfs*24
G127X I
G127X II
G93A
D90A
L117V
A4V
H46R
N86S
E78_R79insSI
Controls
Mutations in other genes
SOD1 mutations
E
19% O2
1% O2
Misfolded SOD1 (µU/mg protein)
Ratio to 19 % O2
A4V
Primary astrocytes

Figure 3

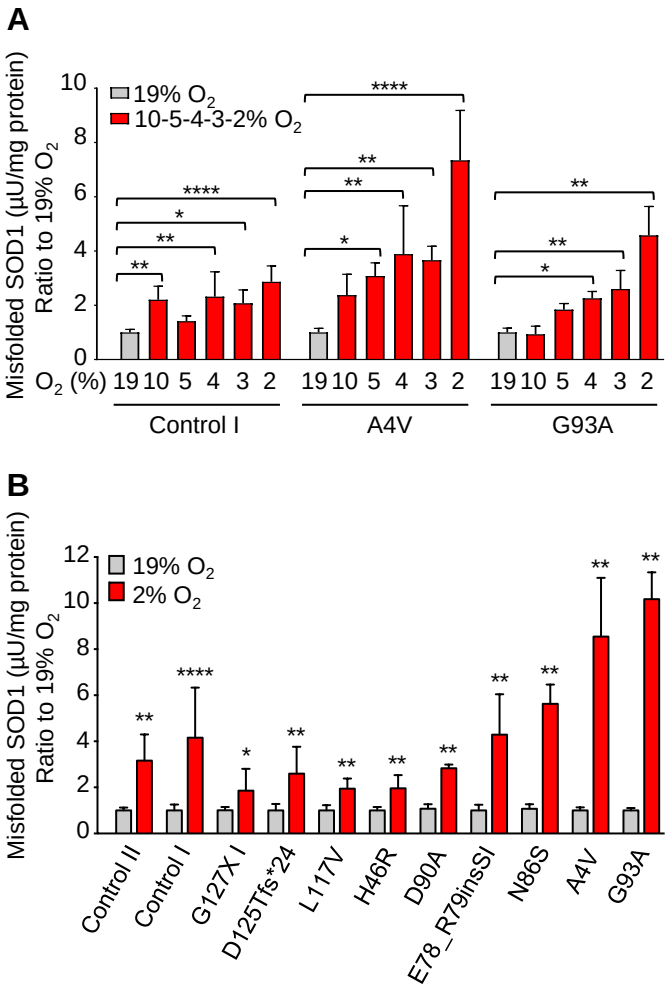
A
Misfolded SOD1 (µU/mg protein)
Ratio to 19% O2
19% O2
10-5-4-3-2% O2
O2 (%) 19 10 5 4 3 2 19 10 5 4 3 2 19 10 5 4 3 2
Control I
A4V
G93A
B
Misfolded SOD1 (µU/mg protein)
Ratio to 19% O2
19% O2
2% O2
Control II
Control I
G127X I
D125Tfs*24
L117V
H46R
D90A
E78_R79insSI
N86S
A4V
G93A

Figure 4

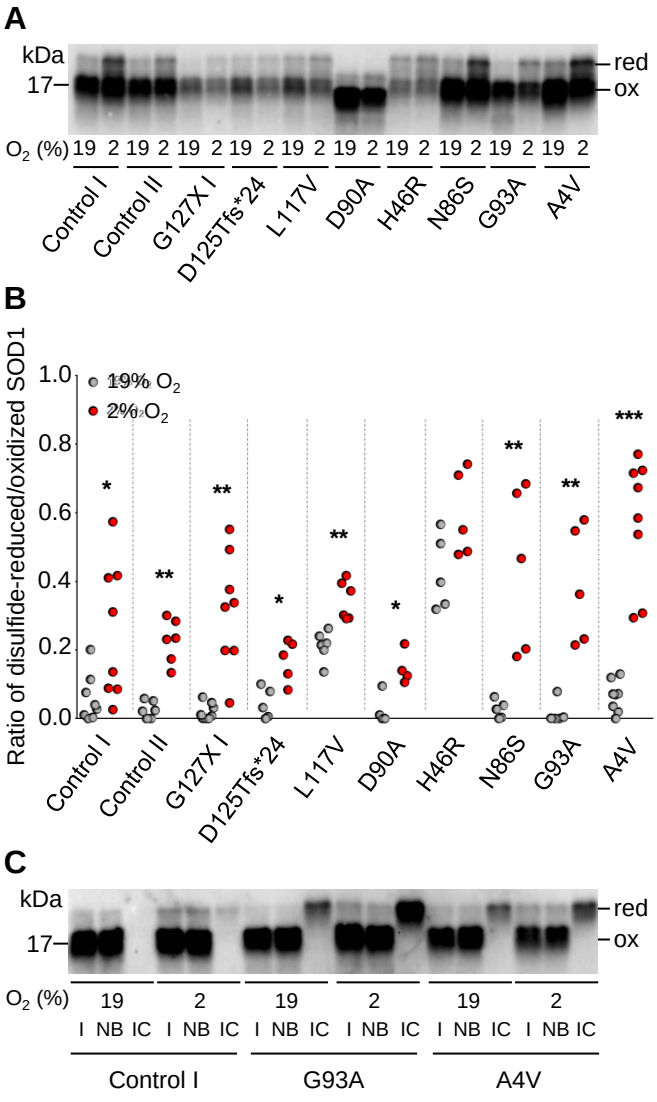
A
kDa
17
red
ox
O2 (%) 19 2 19 2 19 2 19 2 19 2 19 2 19 2 19 2 19 2 19 2
Control I
Control II
G127X I
D125Tfs*24
L117V
D90A
H46R
N86S
G93A
A4V
B
Ratio of disulfide-reduced/oxidized SOD1
19% O2
2% O2
1.0
0.8
0.6
0.4
0.2
0.0
*
**
**
*
**
*
**
**
***
Control I
Control II
G127X I
D125Tfs*24
L117V
D90A
H46R
N86S
G93A
A4V
C
kDa
17
red
ox
O2 (%) 19 2 19 2 19 2
I NB IC I NB IC I NB IC I NB IC I NB IC I NB IC
Control I
G93A
A4V

Figure 5

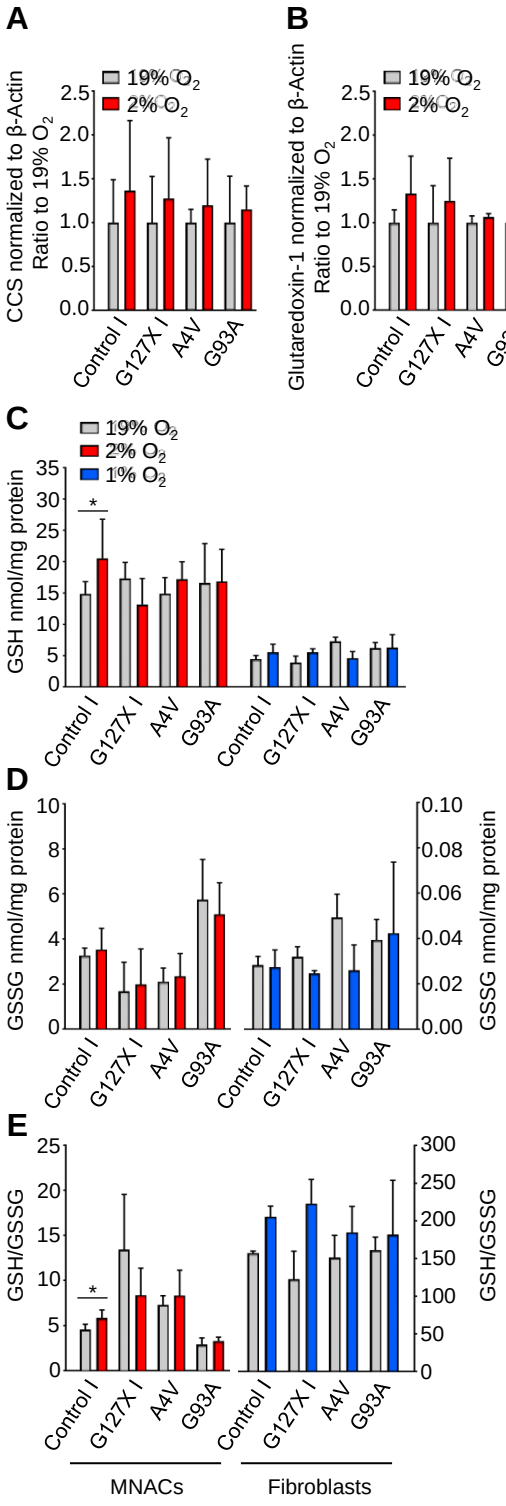
A
CCS normalized to β-Actin
Ratio to 19% O2
19% O2
2% O2
Control I
G127X I
A4V
G93A
B
Glutaredoxin-1 normalized to β-Actin
Ratio to 19% O2
C
GSH nmol/mg protein
1% O2
D
GSSG nmol/mg protein
E
GSH/GSSG
MNACs
Fibroblasts

Figure 6

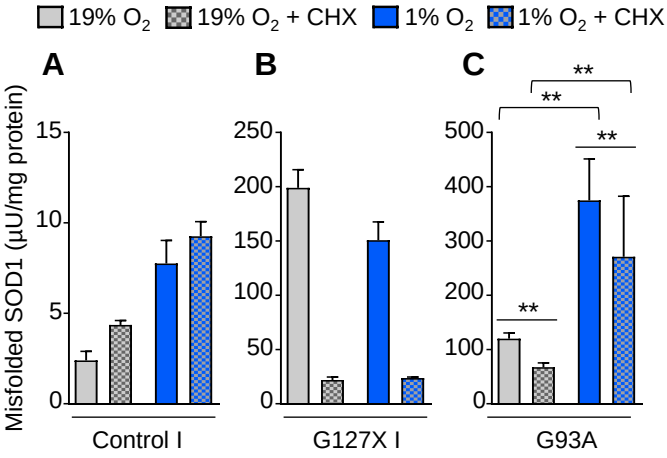
19% O2
19% O2 + CHX
1% O2
1% O2 + CHX
A
B
C
Misfolded SOD1 (µU/mg protein)
15
10
5
0
250
200
150
100
50
0
500
400
300
200
100
0
**
**
**
**
Control I
G127X I
G93A

Figure 7

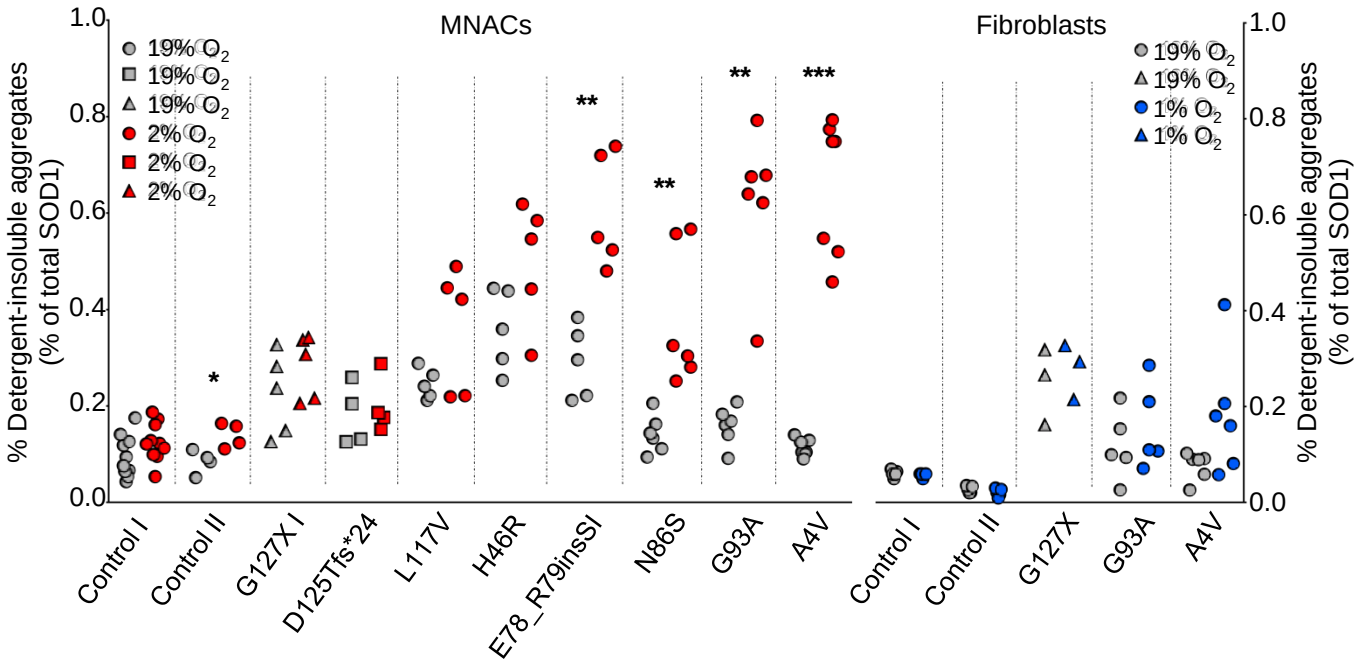
MNACs
Fibroblasts
% Detergent-insoluble aggregates (% of total SOD1)
19% O2
19% O2
19% O2
2% O2
2% O2
2% O2
1% O2
1% O2
1.0
0.8
0.6
0.4
0.2
0.0
*
**
**
**
***
Control I
Control II
G127X I
D125Tfs*24
L117V
H46R
E78_R79insSI
N86S
G93A
A4V
Control I
Control II
G127X
G93A
A4V